Compact-envelope bright solitary wave in a DNA double strand

P. B. Ndjoko,[1,2] J. M. Bilbault,[1] S. Binczak,[1] and T. C. Kofane[2]
[1]*Laboratoire LE2I, Université de Bourgogne UMR CNRS 5158, B.P. 47870, 21078 Dijon Cedex, France*
[2]*Laboratoire de mécanique, Département de Physique, Faculté de Sciences,Université de Yaoundé I, P.B. 812, Yaoundé, Cameroon*
(Received 13 April 2011; revised manuscript received 8 December 2011; published 26 January 2012)

We study the nonlinear dynamics of a homogeneous DNA chain that is based on site-dependent finite stacking and pairing enthalpies. We introduce an extended nonlinear Schrödinger equation describing the dynamics of modulated wave in DNA model. We obtain envelope bright solitary waves with compact support as a solution. Analytical criteria of existence of this solution are derived. The stability of bright compactons is confirmed by numerical simulations of the exact equations of the lattice. The impact of the finite stacking energy is investigated, and we show that some of these compact bright solitary waves are robust, while others decompose very quickly depending on the finite stacking parameters.

DOI: 10.1103/PhysRevE.85.011916 PACS number(s): 87.14.gk, 02.70.−c, 45.20.Jj, 87.15.H−

I. INTRODUCTION

The dynamics of DNA has been extensively studied during the last decade. Particularly, the nonlinear field of sciences pays special attention to the processes that take place at the base pair scale [1]. The local opening of the DNA double helix at the transcription start site is a crucial step for the genetic code. This opening is driven by proteins, but the intrinsic fluctuations of DNA itself probably play an important role. The dynamical properties of these bubbles and their relations to biological functions have therefore been the subject of many experimental and theoretical studies. To understand the phenomenon of thermal denaturation and the dynamics in DNA, Peyrard and Bishop (PB) have proposed a model where DNA is represented by a pair of harmonic chains coupled by a nonlinear potential (Morse potential) [1,2]. This model describes, in a simplified way, the hydrogen bond and has been used successfully in numerous applications such as energy localization [3] or to calculate solitonic speed [4]. Experiments proved that the free energy of opening base pairs depends on the identity of the next base pairs; this is due to the stacking interaction between neighboring bases on the same strand [5]. As is well known, the solitons existing in the PB model result from the balanced competition between dispersion and nonlinear effects. In the huge taxonomy of the models for DNA dynamics, the possibility that nonlinear effects might focus the vibrational energy of DNA into localized coherent structures is indeed expressed by considering pulse waves, kinks, or breathers [6]. By means of a small amplitude expansion in the original PB model, the classical nonlinear Schrödinger (NLS) equation is retrieved. Recently, it has been shown that the inclusion of anharmonicities in the study of lattice models can produce qualitatively new effects. In particular, Rosenau and Hyman [7] found solutions of the solitary type without infinite tails, termed solitons with compact support or compactons. These traveling-wave solutions have a remarkable property: Unlike the Korteweg de Vries (KdV) soliton, which narrows as the amplitude increases, the compacton's width is independent of the amplitude [8]. As a consequence, two adjacent compactons do not interact unless they come into contact in a way similar to the contact between hard spheres [9,10]. Note that the stacking interaction in the Dauxois-Peyrard-Bishop (DPB) [11] model is not harmonic, but it still differs fundamentally from that of statistical models because it does not make reference to any characteristic energy. Since its introduction, this model has been used to unravel several aspects of melting. Joyeux and Buyukdagli (JB) [12] proposed a few years ago a dynamical model for DNA, which is closer to the statistical ones than the DPB model, in the sense that it is based on site-specific stacking enthalpies and showed that the finiteness of the stacking interaction is, in itself, sufficient to ensure a sharp melting transition.

In the present work, we show that this finite stacking energy interaction model supports envelope bright solitary waves with compact support. To this end, the organization of the paper is as follows. In Sec. II, we present the model and its equations. In Sec. III, by means of the semidiscrete approximation, we derive the extended NLS equation governing modulated waves in the lattice. Exact analytical solution with compact support is obtained for this extended NLS equation in Sec. IV. Numerical investigations are considered in order to verify the validity and the stability of analytical predictions, and we draw our conclusions in Sec. V.

II. MODEL AND EQUATION OF MOTION

The general form of the model we are considering in this paper is

$$H = \sum_n \frac{1}{2m} P_n^2 + W(y_n, y_{n-1}) + D(e^{(-\alpha y_n)} - 1)^2, \quad (1)$$

where we choose the JB model [see the finite stacking potential in Fig. 1(a)], i.e.,

$$W(y_n, y_{n-1}) = \frac{\triangle H_n}{C}(1 - e^{-b(y_n - y_{n-1})^2}) + K_b(y_n - y_{n-1})^2, \quad (2)$$

where $\Delta H_n/C$ is a Gaussian hole of depth and the backbone stiffness is taken as a harmonic potential of constant K_b. In this set of equations, m is the reduced mass of the bases, and y_n is the displacement that stretches the hydrogen bonds. The last term in Eq. (1) is the on-site Morse potential [see Fig. 1(b)], where D denotes the dissociation energy, and the parameter α, homogeneous to the inverse of a length, sets the special scale of the potential. This on-site Morse potential appears as a

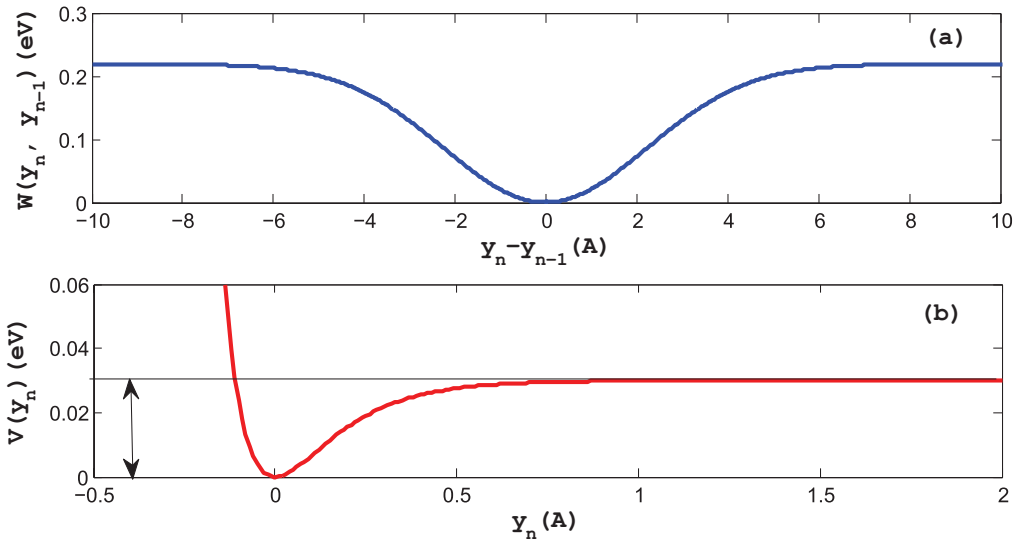

FIG. 1. (Color online) (a) Representation of the stacking interaction potential of base pairs $W(y_n, y_{n-1})$ defined by the JB model as a function of the relative displacement $y_n - y_{n-1}$. $K_b = 10^{-5}$ eV A^{-2} being very small, its effect on infinite behavior (when $y_n - y_{n-1} \to \infty$) is not visible here. (b) Morse potential with the dissociation energy.

"substrate" potential in the model, which comes directly from the structure of DNA. In this work numerical values of our parameters are those of Refs. [12,13], that is, $m = 300$ amu, $D = 0.04$ eV, $\alpha = 4.45$ Å^{-1}, $K_b = 10^{-5}$ eV Å^{-2}. Including Eq. (2) in (1) yields the corresponding equation of motion of the nth base pair:

$$\frac{d^2y_n}{dt^2} = \frac{2K_b}{m}(y_{n+1} + y_{n-1} - 2y_n) + \frac{2b\triangle H_n}{mC}\left[(y_{n+1} - y_n) \times e^{-b(y_{n+1}-y_n)^2} - (y_n - y_{n-1})e^{-b(y_n - y_{n-1})^2}\right] + \frac{2\alpha D}{m}e^{(-\alpha y_n)}(e^{-\alpha y_n} - 1). \quad (3)$$

According to the original approach of Ref. [14], it is assumed that the oscillations of bases are large enough to be anharmonic, but still insufficient to break the bond since the plateau of the Morse potential is not reached. Thus, it is presumed that the base nucleotides oscillate around the bottom of the Morse potential. We can therefore expand the exponential function up to the third-order approximation. Finally, Eq. (3) becomes

$$\frac{d^2y_n}{dt^2} = \left(\frac{2K_b}{m} + \frac{2b\triangle H_n}{mC}\right)(y_{n+1} + y_{n-1} - 2y_n) - \frac{2b^2\triangle H_n}{mC}\left[(y_{n+1} - y_n)^3 - (y_n - y_{n-1})^3\right] - \frac{2\alpha^2 D}{m}\left(y_n - \frac{3}{2}\alpha y_n^2 + \frac{7}{6}\alpha^2 y_n^3\right). \quad (4)$$

On the other hand, it is convenient for the analytical and numerical calculations to transform these equations into a dimensionless form by defining the dimensionless variables

$$Y_n = \alpha y_n, \quad \tau = (\sqrt{D\alpha^2/m})t, \quad C_l = \frac{2}{D\alpha^2}\left(K_b + \frac{b\triangle H_n}{C}\right), \quad C_{nl} = -\frac{2}{D\alpha^4}\frac{b^2\triangle H_n}{C}, \quad (5)$$

which transforms Eq. (4) into

$$\frac{d^2Y_n}{d\tau^2} = C_l(Y_{n+1} + Y_{n-1} - 2Y_n) + C_{nl}\left[(Y_{n+1} - Y_n)^3 - (Y_n - Y_{n-1})^3\right] - \omega_g^2\left(Y_n - \frac{3}{2}Y_n^2 + \frac{7}{6}Y_n^3\right), \quad (6)$$

where $\omega_g^2 = 2$. Note that the control parameters b and $\Delta H_n/C$ allow one to fix independently C_l and C_{nl}.

For finite wave amplitude, nonlinearities of the system give rise to the generation of higher harmonics. However, we are using the so-called rotating-wave approximation, which consists essentially in neglecting harmonics, and we substitute into Eq. (6) the trial solution [15,16]

$$Y_n(\tau) = B(X,T)e^{i\theta_n} + B^*(X,T)e^{-i\theta_n}, \quad (7)$$

where the asterisk denotes complex conjugation. This expression of $Y_n(\tau)$ includes the fast local oscillation through the dependence of the phase $\theta_n = kn - \omega\tau$, and then preserves the discrete character of the system [17], while the dependence of the envelope part is described by the slow amplitude variation of the function $B(X,T)$ with respect to the slow variables $T = \varepsilon^2\tau$ and $X = \varepsilon(n - v_g\tau)$, ε being a small dimensionless parameter. Here the lattice spacing has been taken as equal to unity. The parameter is the group velocity associated to the wave packet. The linear oscillation frequency of the base pairs and wave number are related $v_g = \frac{d\omega}{dk}$ by the dispersion equation

$$\omega^2 = \omega_g^2 + 4C_l\sin^2(k/2). \quad (8)$$

As shown by Eq. (8), the linear equation has a gap ω_g and is limited by the cutoff frequency $\omega_m = \sqrt{\omega_g^2 + 4C_l}$ due to the discreteness, whereas $v_g = \frac{C_l\sin(k)}{\omega}$. Instead of applying the standard reductive perturbation method in the semidiscrete limit to Eq. (6), which forbids one from appreciating the role of the nonlinear dispersion in Eq. (6), we substitute Eq. (7) into

Eq. (6) and neglect all terms in ε^5 or more [15,18]. Then this envelope part leads to the following one-dimensional NLS:

$$
\begin{aligned}
& i\frac{\partial B}{\partial T} + PB_{XX} + Q|B|^2B \\
& = \frac{C_{nl}}{w}\Big\{il_1[|B|^2B_X] + il_2[B^*B_XB_{XX}] + 2il_3[|B_X|^2B_X \\
& + BB_XB^*_{XX} + BB^*_XB_{XX}] + l_4\left[B|B_X|^2 + \frac{1}{2}B^2B^*_{XX}\right] \\
& + l_5[|B|^2B_{XX}] + 4l_6\big[B^*B^2_X\big] + l_7\big[B^2_XB^*_{XX} \\
& + 2|B_X|^2B_{XX}\big]\Big\}. \qquad (9)
\end{aligned}
$$

The terms proportional to l_k with $k = 1, 2, 3, \ldots, 7$ result from the inclusion of the finite stacking energy. They therefore include the effect of nonlinear dispersion terms. The different expressions involved in (9), including the group velocity dispersion (GVD) P and the self-phase modulation (SPM) Q depend on k, ω, C_l, and C_{nl}:

$$
\begin{aligned}
P &= \frac{C_l\cos(k) - v_g^2}{2\omega}, \\
Q &= -\frac{1}{2\varepsilon^2\omega}\left[\frac{7}{6}\omega_g^2 + 48C_{nl}\sin^4\left(\frac{k}{2}\right)\right], \\
l_1 &= -\frac{24}{\varepsilon}\sin(k)\sin^2\left(\frac{k}{2}\right), \\
l_2 &= -3\varepsilon\left[\sin(k) + \sin(2k)\right], \qquad (10) \\
l_3 &= -\frac{3\varepsilon\sin(k)}{2}, \qquad l_4 = 12\sin^2\left(\frac{k}{2}\right), \\
l_5 &= -12\sin^2\left(\frac{k}{2}\right)\cos(k), \\
l_6 &= -\frac{3\sin\left(\frac{k}{2}\right)\sin\left(\frac{3k}{2}\right)}{2}, \quad l_7 = \frac{3\varepsilon^2\cos(k)}{2}.
\end{aligned}
$$

Assuming that $B(X,T)$ and all its derivative converge to zero sufficiently rapidly as $X \longrightarrow \pm\infty$, Eq. (9) has two conservation laws, which can be expressed in terms of continuity equations. The first conserved quantity is the Hamiltonian $H = \int \hat{H}dX$ corresponding to invariance under translations in X, where the Hamiltonian density is

$$\hat{H} = \hat{H}_1 + \hat{H}_2 + \hat{H}_2^*, \qquad (11)$$

with

$$\hat{H}_1 = -P|B_X|^2 + \frac{Q}{2}|B|^4 + \frac{3l_7C_{nl}}{2\omega}|B_X|^4 - l_5\big[|B|^2|B_X|^2\big], \qquad (12)$$

$$
\begin{aligned}
\hat{H}_2 = \frac{C_{nl}}{\omega}\Big\{ & \frac{il_1}{2}[|B|^2BB^*_X] + \frac{il_2}{4}[B^*|B_X|^2B_X] \\
& + \frac{il_3}{2}[|B_X|^2B^*_X] + \frac{3l_4}{4}\big[B^2B^{*2}_X\big] + 2l_6\big[B^{*2}B^2_X\big]\Big\}. \qquad (13)
\end{aligned}
$$

The second important invariant is the normalization of the envelope

$$N = \int |B|^2dX. \qquad (14)$$

The conservation of norm is intimately connected to the phase invariance of Eq. (9), i.e., the fact that if $\{B\}$ is a solution so is $\{Be^{i\varphi}\}$ for any constant phase $\varphi \in \mathbb{R}$.

III. BRIGHT SOLITONS WITH COMPACT SUPPORT SOLUTION

The existence of compact waves has been rigorously proven by Saccomandi and Sgura [19] for Hamiltonian systems, provided that an anharmonicity condition is fulfilled. To proceed with the integration of the extended NLS equation (9), we first separate the complex envelope function and the phase shift [15] $\xi(X,T)$ according to

$$B(X,T) = \phi(X,T)\exp[-i\xi(X,T)], \qquad (15)$$

where ϕ and ξ are real functions of X and T. From the analysis of the coefficients l_k with $k = 1, 2, 3, \ldots, 7$, it appears that $8l_6 = 2l_5 - l_4$. By using this relation and substituting the expression (15) into Eq. (9), we obtain a nonlinear system of two equations by separating real and imaginary parts. It, respectively, reads

$$
\begin{aligned}
-\left[\frac{\partial\xi}{\partial T} + P\left(\frac{\partial\xi}{\partial X}\right)^2\right]\phi + P\frac{\partial^2\phi}{\partial X^2} + Q\phi^3 = \frac{C_{nl}}{\omega}\Bigg\{ & -\left[l_1\frac{\partial\xi}{\partial X} + 8l_6\left(\frac{\partial\xi}{\partial X}\right)^2 + (l_2 - 2l_3)\left(\frac{\partial\xi}{\partial X}\right)^3\right]\phi^3 \\
& - \left[3l_7\left(\frac{\partial\xi}{\partial X}\right)^4\right]\phi^3 + (l_4 + 4l_6)\left[\phi^2\frac{\partial^2\phi}{\partial X^2} + \phi\left(\frac{\partial\phi}{\partial X}\right)^2\right] \qquad (16) \\
& - \left[(2l_2 + 2l_3)\frac{\partial\xi}{\partial X} - 5l_7\left(\frac{\partial\xi}{\partial X}\right)^2\right]\phi\left(\frac{\partial\phi}{\partial X}\right)^2 \\
& - \left[l_2\frac{\partial\xi}{\partial X} - l_7\left(\frac{\partial\xi}{\partial X}\right)^2\right]\phi^2\frac{\partial^2\phi}{\partial X^2} + 3l_7\left(\frac{\partial\phi}{\partial X}\right)^2\frac{\partial^2\phi}{\partial X^2}\Bigg\},
\end{aligned}
$$

$$
\begin{aligned}
\frac{\partial\phi}{\partial T} + 2P\frac{\partial\xi}{\partial X}\frac{\partial\phi}{\partial X} = \frac{C_{nl}}{\omega}\Bigg\{ & \left[l_1 + 16l_6\frac{\partial\xi}{\partial X} - (l_2 - 10l_3)\left(\frac{\partial\xi}{\partial X}\right)^2 - 6l_7\left(\frac{\partial\xi}{\partial X}\right)^3\right]\phi^2\frac{\partial\phi}{\partial X} \\
& + \left[2l_3 + 2l_7\frac{\partial\xi}{\partial X}\right]\left(\frac{\partial\phi}{\partial X}\right)^3 + \left[l_2 + 4l_3 + 2l_7\frac{\partial\xi}{\partial X}\right]\phi\frac{\partial\phi}{\partial X}\frac{\partial^2\phi}{\partial X^2}\Bigg\}. \qquad (17)
\end{aligned}
$$

Let us look for traveling wave solutions in the form $\phi(X,T)=\phi(z)$ with $z=(X-v_eT)$ and linear phase shift $\xi(X,T)=\gamma(X-v_\phi T)$, where v_e and v_ϕ are the envelope and phase velocities, respectively. We can simplify Eqs. (16) and (17) by considering the following equations:

$$\phi_T=-v_e\phi_z,\ \phi_X=\phi_z, \tag{18}$$

which reduces straightforwardly Eq. (17) to

$$\frac{C_{nl}}{\omega}\left\{[l_2+4l_3+2l_7\gamma]\phi\frac{d^2\phi}{dz^2}+2(l_3+l_7\gamma)\left(\frac{d\phi}{dz}\right)^2 +[l_1+16l_6\gamma-(l_2-10l_3)\gamma^2-6l_7\gamma^3]\phi^2\right\} +v_e-2P\gamma=0. \tag{19}$$

By using the drop boundary conditions

$$\phi\to 0,\ \phi_z\to 0 \text{ at } z\to\pm\infty, \tag{20}$$

we obtain

$$v_e=2P\gamma. \tag{21}$$

The first integration of Eq. (16) gives

$$\eta_1\left(\frac{d\phi}{dz}\right)^4+(\eta_2+\eta_3\phi^2)\left(\frac{d\phi}{dz}\right)^2+\eta_4\phi^4+\eta_5\phi^2=0, \tag{22}$$

where

$$\eta_1=\frac{3C_{nl}}{4\omega}l_7;\ \eta_2=-\frac{P}{2};\ \eta_3=\frac{C_{nl}}{2\omega}(l_4+4l_6-l_2\gamma+l_7\gamma^2),$$
$$\eta_4=-\frac{1}{4}\left\{Q+\frac{C_{nl}}{\omega}[l_1\gamma+8l_6\gamma^2+(l_2-2l_3)\gamma^3-3l_7\gamma^4]\right\},$$
$$\eta_5=\frac{\gamma}{2}(P\gamma-v_\phi),$$
$$\gamma=\frac{l_2+2l_3}{4l_7}. \tag{23}$$

Equation (22) leads to

$$\left(\frac{d\phi}{dz}\right)^2=-\frac{(\eta_2+\eta_3\phi^2)}{2\eta_1}+\frac{\sqrt{(\eta_3^2-4\eta_1\eta_4)\phi^4+(2\eta_2\eta_3-4\eta_1\eta_5)\phi^2+\eta_2}}{2\eta_1}, \tag{24a}$$

or

$$\left(\frac{d\phi}{dz}\right)^2=-\frac{(\eta_2+\eta_3\phi^2)}{2\eta_1}-\frac{\sqrt{(\eta_3^2-4\eta_1\eta_4)\phi^4+(2\eta_2\eta_3-4\eta_1\eta_5)\phi^2+\eta_2}}{2\eta_1}. \tag{24b}$$

Taking the phase velocity as

$$v_\phi=\frac{v_e}{2}-\frac{\eta_2\left(\eta_3+\sqrt{\eta_3^2-4\eta_1\eta_4}\right)}{\eta_1\gamma}, \tag{25}$$

Eqs. (24a) and (24b), respectively, take a simpler form:

$$\left(\frac{d\phi}{dz}\right)^2=\mu^2(B_0^2-\phi^2), \tag{26a}$$

$$\text{and}\quad \left(\frac{d\phi}{dz}\right)^2=-\frac{\eta_4}{\eta_1\mu^2}\phi^2, \tag{26b}$$

with

$$B_0^2=\left(\frac{P}{\eta_3-\sqrt{\eta_3^2-4\eta_1\eta_4}}\right), \tag{27}$$

and

$$\mu^2=\left(\frac{\eta_3-\sqrt{\eta_3^2-4\eta_1\eta_4}}{2\eta_1}\right). \tag{28}$$

For the resolution of this equation, we use the same technique as in Refs. [20,21]. The integration of Eq. (26a) yields the following solution in the compact support:

$$\phi(z)=B_0\cos\mu(z-z_0),\ \text{if}\ |(z-z_0)3\leqslant\pi/2\mu, \tag{29}$$

while in the noncompact domain, $\phi(z)=0$, which respects Eq. (26b). The parameter μ may serve as a measure of the importance of discreteness effect in the system. This solution indicates that the compact bright solitary wave is characterized by amplitude B_0 and a strictly limited width $L=\pi/\mu$. Moreover, z_0 locates the center of mass of the solution. Note that other solutions of (26a) exist, describing multicompacton waves, such as $\phi(z)=B_0\cos\mu(z-z_0)$ if $|(z-z_0)|\leqslant\pi/\mu$, and 0 elsewhere, i.e., a double compacton solution (see Sec. IVA). Gaeta *et al.* [22] combined also two (or more) kink solutions to obtain a multikink solution, which is a special type of multicompacton solution, but they considered a periodic on-site potential leading to an arbitrary sequence of kinks and antikinks. According to Eqs. (27) and (28), the

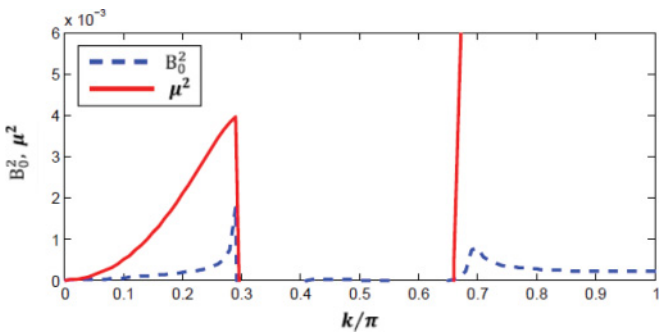

FIG. 2. (Color online) Study of the existence criteria of compact bright solitary waves as a function of the wave vector k for the parameter $D=0.04$ eV, $\alpha=4.45$ Å^{-1}, $K_b=10^{-5}$eV Å^{-2}, $\Delta H_n/C=0.22$ eV. [Solid line corresponds to the criterion obtained from Eq. (32) and dashed line for the one obtained from Eq. (33)]. It appears that the criteria are satisfied in the same domains of the wave vector.

existence of the compact solution (29) is subjected to the constraints

$$\frac{P}{\eta_3 - \sqrt{\eta_3^2 - 4\eta_1\eta_4}} \geqslant 0, \tag{30}$$

$$\frac{\eta_3 - \sqrt{\eta_3^2 - 4\eta_1\eta_4}}{2\eta_1} \geqslant 0. \tag{31}$$

The left-hand side of these criteria of existence (30) and (31) of a compact solitary wave are calculated as a function of the wave number and sketched in Fig. 2. From this figure, it appears that the criteria (30) and (31) are satisfied for the same domain of wave numbers, that is, in $[0,0.29\pi]$ and $[0.65\pi,\pi]$. Moreover, B_0^2 and μ^2 admit a maximum for a value very close to the upper boundary of the first of these domains. These constraints can be rewritten in terms of the frequency ω of the carrier wave by means of the dispersion relation (8). By replacing the parameters η_i by their expressions in Eq. (23), the existence condition of a compact bright solitary wave becomes

$$-r < C_{nl} < 0, \tag{32}$$

with

$$r = \frac{(7/6)\omega_g^2}{12\sin^4(k/2) - (1/8)[l_1\gamma + 8l_6\gamma^2 + (l_2 - 2l_3)\gamma^3 - 3l_7\gamma^4]}. \tag{33}$$

We remark that this criterion is independent of the GVD in the formation of this compact bright solitary wave. However, it appears from Eqs. (23) and (25) that the GVD controls the compact solitary wave's speed. Equations (30) and (31) show also that the existence of the compact solitary wave in the network is closely connected to the presence of the nonlinear dispersive terms proportional to coefficients η_1 and η_3. It is possible to obtain the compact solution even if the self-phase modulation SPM term is absent ($Q = 0$). Accordingly, the SPM term plays a minor role in the formation of the compact envelope bright solitary wave.

We then check whether this solution is a maximum or a minimum of the effective Hamiltonian of the system. In fact, from the study of the nonlinear extended KdV equation, it has been proved that when the effective Hamiltonian is maximum (resp. minimum), the compacton solution turns out to be unstable (resp. stable) [23]. Thus the effective Hamiltonian can be a simple way of checking stability. We insert in the Hamiltonian (11), by means of Eqs. (15) and (29), the following compact form as a trial function:

$$B_0 \cos\mu(z - z_0)\exp[i\gamma(X - v_\phi\tau)], |(z - z_0)| \leqslant \pi/2\mu, \tag{34}$$

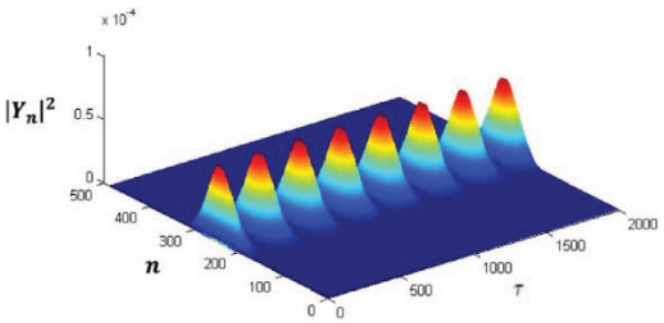

FIG. 3. (Color online) Temporal behavior of compacton (initial speed equal zero) spacial profile. Magnitude $A_0 = 0.015$, width $L = 50$, and central site located at $n_0 = N/2$. The solution is stable.

where B_0 and μ are now taken as free parameters. Taking into account the relationships (11), (12), and (13), we obtain the following contribution for the compact region of the wave ($|(z - z_0)| \leqslant \pi/2\mu$) in the effective Hamiltonian:

$$H_C = \frac{3\pi B_0^4}{8\mu}\left\{\frac{3l_7}{2}[\mu^4 + \gamma^4] - \frac{4\pi P}{3B_0^2}[\mu^2 + \gamma^2] + \mu^2\left[l_7\gamma^2 + \frac{l_1}{12}\gamma + \frac{l_4}{3} + \frac{2l_5}{3}\right] + \left[\frac{Q}{2} + \frac{l_1}{4}\gamma(1 + \gamma^2)\right]\right\}. \tag{35}$$

Due to the fact that solution (34) satisfies the normalization condition (14), the problem of minimizing H under the constraint $N = \text{const}$ is reduced to the problem of satisfying the equation $\frac{\partial H}{\partial \mu} = 0$, and we find that the Hamiltonian H has a minimum at the exact value of μ for fixed N, which indicates the stability of the analytical compact wave (34).

IV. DIRECT NUMERICAL ANALYSIS

The results discussed in the previous section are only approximated ones since they are obtained not from the initial equations of motion (3) but from the extended NLS equation (9) derived after some hypothesis. In order to check if the above analytic continuum bright soliton with compact support can survive in the discrete lattice, different numerical simulations of Eq. (3) have been performed, using the following initial condition:

$$Y_n(t = 0) = \begin{cases} A_0 \cos\mu(n - n_0)\exp[i(k - \gamma)n], & |(n - n_0)| \leqslant \pi/2\mu \\ 0 & \text{otherwise,} \end{cases} \tag{36}$$

obtained from Eqs. (7), (15), and (29). The system has been integrated with a fourth-order Runge-Kutta scheme with a time

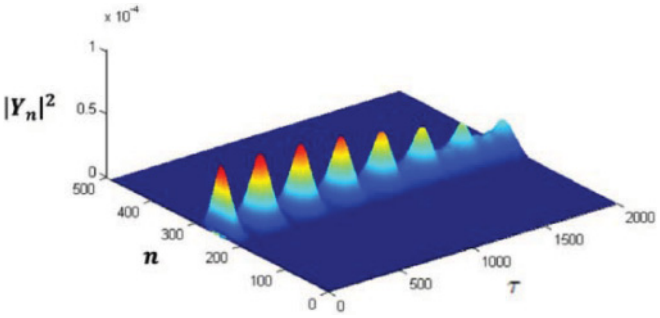

FIG. 4. (Color online) Same as in Fig. 3 but the initial envelope width is now $L = 22$. The initial compacton loses its shape.

step chosen to conserve the energy to an accuracy better than 10^{-6} over a complete run. The number of base pairs is fixed at $N = 600$ in order to avoid any wave reflection at the end of the molecule that can affect the creation process and the dynamics of the localized structures.

A. Stability of the compact static wave

To check the stability of the solutions over time, the solution is evolved over a very long time. First, the initial velocity is taken to be zero; i.e., from Eqs. (7), (8), (18), and (21), $v_g + v_e = 0$ (see Sec. IV B). Figure 3 shows the stability of the lattice profile of the bright soliton with compact envelope over 2000 normalized time units (4.2×10^{-12}s), which is much greater than the typical time scale of the transversal movements in DNA (10^{-14}s). The initial width and amplitude of compactons are chosen to be respectively $L = \pi\mu = 50$ times the lattice spacing, and $A_0 = 2B_0 = 0.015$, where B_0 and μ are, respectively, given by Eqs. (27) and (28). As can be seen from this figure, the initial analytic continuum compact envelope solutions of Eq. (29) remains stable even after a very long time in the discrete lattice. We have also considered the compact envelope solution with width $L = 22$. In this case, the results of the numerical simulations show that although the solution remains stable after 500 time units, it loses its compact support and develops some structures near its edge after a larger time: 1000 time units (it starts developing a tail near the edge of the compacton, thereby destroying the compact nature of the solutions; see Fig. 4). It is clear that the stability of the compacton solutions with initial speed equal to zero, in a discrete lattice, depends crucially on its width which measures the discreteness effects in the system. Moreover, as can be seen in Ref. [24], the width and the amplitude are some parameters acting on the stability of compact wave with the zero velocity. In order to consider stability against perturbations, we add a small one to the equilibrium solution $Y_n(t) = \hat{Y}_n(t) + \epsilon_n(t)$,

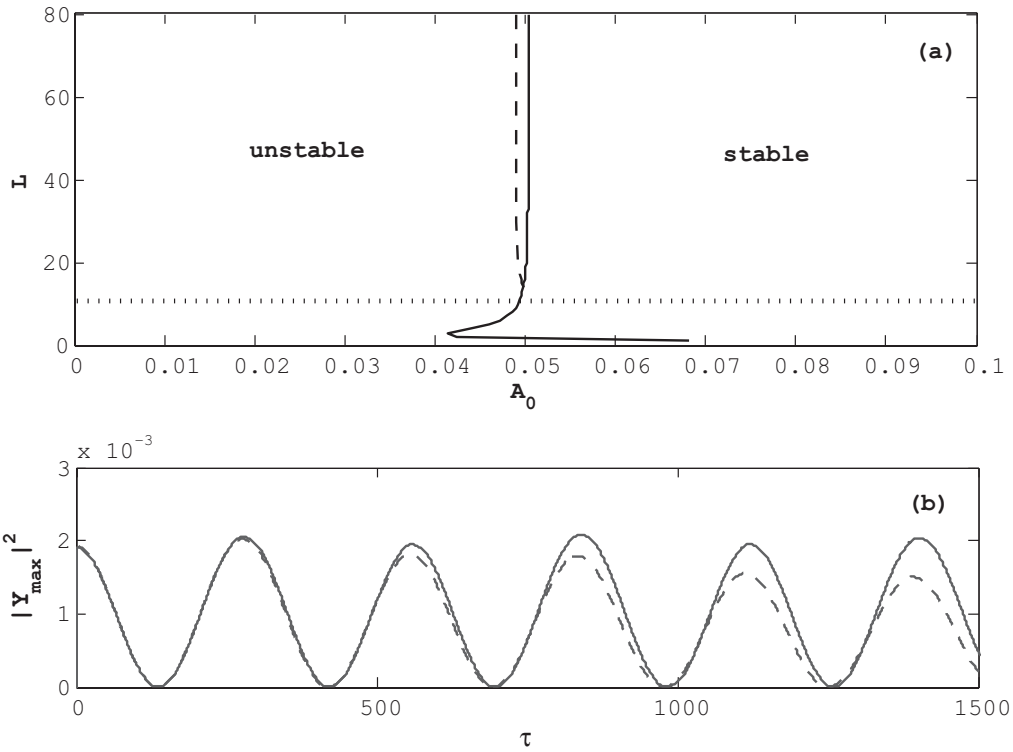

FIG. 5. (a) Regions where the static compact bright solitary wave is stable. The parameters have been chosen as $m = 300$ amu, $D = 0.04$ eV, $\alpha = 4.45$Å^{-1}, $K_b = 10^{-5}$ eV Å^{-2}. Solid line and dashed line show, respectively, the analytical and numerical studies. We note that the stability against small perturbations of the compact solitary wave depends on the amplitude and the width of the initial wave. Our analytical and numerical studies show that in the left region, there exist values of q revealing instabilities, while in the right region, no instability appears, whatever the value of q. In addition, the dotted line demarcates the region of width where the continuum approximation is not correct. (b) The initial pulse breaks up into a pulse train, and the amplitude decreases as the time increases, when the perturbation wave number does not respect the condition of Eq. (41).

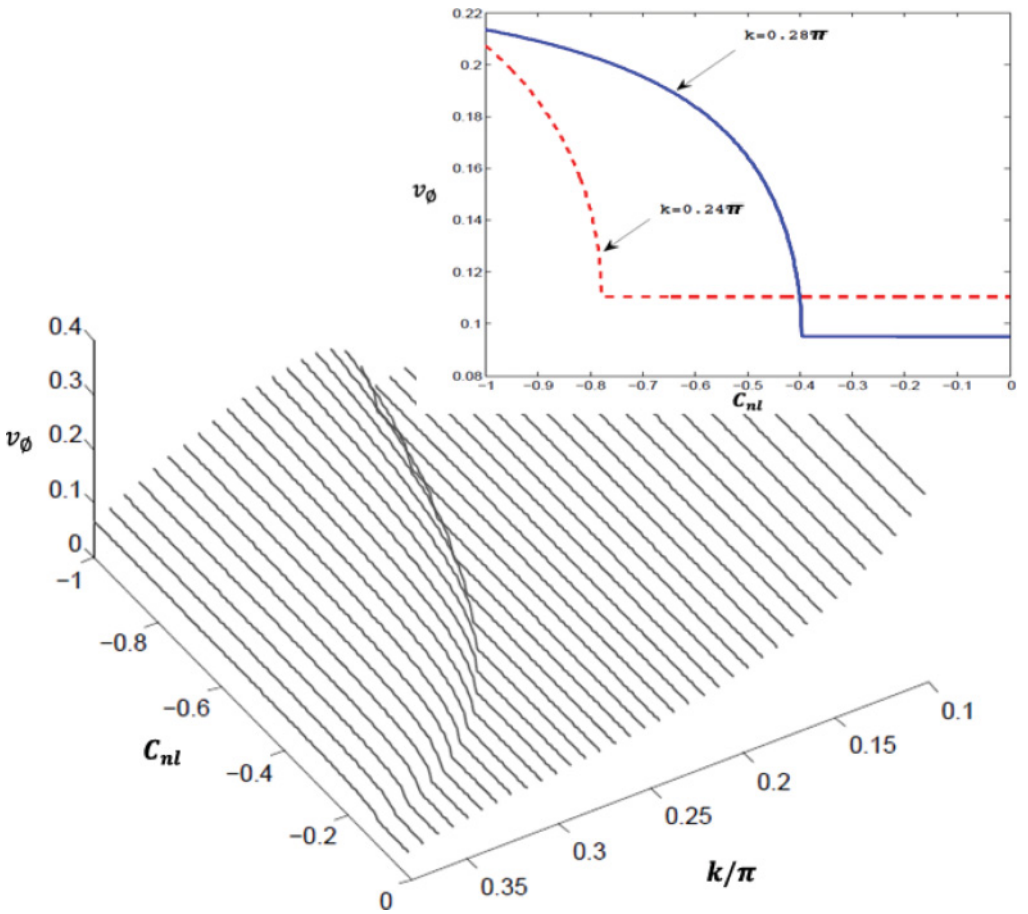

FIG. 6. (Color online) Variation of phase velocity vs negative anharmonicity parameter C_{nl} and wave number k. In insert, two values of wave numbers are chosen: $k = 0.28\pi$ (solid line), $k = 0.24\pi$ (dashed line).

$[\hat{Y}_n(t)$ as given by Eq. (36) when $t = 0]$ and linearize equation of motion Eq. (6) with respect to $\epsilon_n(t)$:

$$\ddot{\epsilon}_n(t) = C_l(\epsilon_{n+1} + \epsilon_{n-1} - 2\epsilon_n) + 3C_{nl}[(\hat{Y}_{n+1} - \hat{Y}_n)^2(\epsilon_{n+1} - \epsilon_n) + (\hat{Y}_{n-1} - \hat{Y}_n)^2(\epsilon_{n-1} - \epsilon_n)] - w_g^2\left(\epsilon_n - 3\hat{Y}_n\epsilon_n + \frac{7}{2}\hat{Y}_n^2\epsilon_n\right). \quad (37)$$

This form was already considered by Gorbach [25] in the case of the compact-like breathers in systems with nonlinear dispersive term. We consider the perturbation in the form $\epsilon_n(t) = b\exp[i(qn - \Omega t)]$ + complex conjugate, q and Ω being wave number and angular frequency of perturbation, respectively. By considering the compact wave at initial position, we obtain the following dispersion relation:

$$\Omega^2 = \left\{4C_l + 12C_{nl}A_0^2[\cos^2(\mu) + 1 - \cos(\mu)\cos(k - \gamma)]\right\} \times \sin^2(q/2) + w_g^2\left(1 - 3A_0 + \frac{7}{2}A_0^2\right). \quad (38)$$

A modulational instability (MI) will develop in the molecule if the right-hand side of this equation is negative; i.e., the perturbed wave can be unstable only if

$$4C_l + 12C_{nl}A_0^2[\cos^2(\mu) + 1 - \cos(\mu)\cos(k - \gamma)] < 0. \quad (39)$$

It becomes possible to express the initial amplitude A_0 with respect to a threshold amplitude $A_{0,\mathrm{cr}}$. Therefore a compact solitary wave introduced in the system stays stable for any q if the initial amplitude exceeds the threshold amplitude $A_{0,\mathrm{cr}}$ defined as follows:

$$A_0 \geqslant A_{0,\mathrm{cr}} = \sqrt{\frac{Cl}{3\,|C_{nl}|}[\cos^2(\mu) + 1 - \cos(\mu)\cos(k - \gamma)]}. \quad (40)$$

This is plotted in Fig. 5(a), where the value of the threshold amplitude $A_{0,\mathrm{cr}}$ depends on the width of compact wave. Even in the unstable region [left part of Fig. 5(a)], the compact wave stays stable if the perturbation wave number q respects the following condition:

$$|\sin(q/2)| \leqslant \sqrt{\frac{w_g^2\left(1 - 3A_0 + \frac{7}{2}A_0^2\right)}{\left|4C_l + 12C_{nl}A_0^2[\cos(\mu)^2 + 1 - \cos(\mu)\cos(k - \gamma)]\right|}}. \quad (41)$$

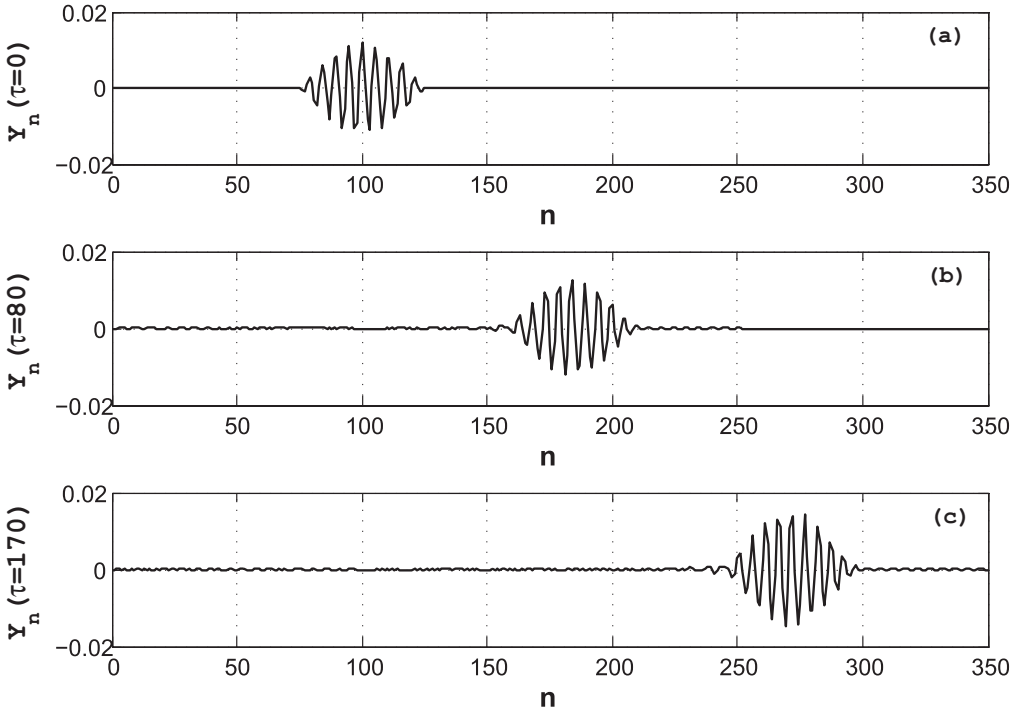

FIG. 7. Time behavior of propagating compact bright solitary wave in DNA for $C_{nl} = -0.4$, i.e., $\Delta H_n/C = 0.22\,\text{eV}$ and $b = 8\,\text{Å}^{-2}$ (a) The initial wave is the compact envelope bright solitary wave located at site $n_0 = 100$ with amplitude $A_0 = 1.2 \times 10^{-2}$, width $L = 50$, and wave number $k = 0.28\pi$. Panels (b) and (c) show the wave at given times of propagation: 80 and 170, respectively. The wave experiences are uniform, and the propagation is stable along the DNA lattice.

Therefore, the stability of the compact solitary waves depends on the parameters of initial compact solitary wave, including the perturbation. For example, by taking the amplitude and width of the initial wave, respectively, as $A = 0.014$ and $L = 50$, the wave suffers eventual destruction when the perturbative wave number is $q = 0.5\pi$ and maintains its stability when the perturbative wave number is $q = 0.07\pi$. For large values of amplitude, the perturbated wave maintains its stability for all values of perturbating wave number, but for smaller amplitudes, as can be seen in Fig. 5(b), the wave predicted to be unstable against MI breaks up into a pulse train, and the amplitude decreases as the time increases.

B. Stability of the compact propagating wave

First, we can see in Eq. (25) that the phase velocity v_ϕ depends on the anharmonicity of the system through η_i. Namely, in Fig. 6, we plot the phase velocity as a function of the anharmonic coefficient C_{nl}. We show that, when $-0.4 \leqslant C_{nl} \leqslant 0$, for k near 0.26π, the phase velocity reaches a minimum value. But the compact wave found as solution of Eq. (6) propagates, in fact, with a speed that is composed of the group velocity v_g and the envelope velocity v_e, given by Eq. (21), that is, $v_C = v_e + v_g$. Fixing initially this velocity to $v_C = 1.00$ cells/normalized time unit (that is, $V_C = 475$ cells/ps in denormalized time unit), which corresponds to Eq. (36) with wave number $k = 0.28\pi$, width $L = 50$, and amplitude $A = 0.012$, we see in Fig. 7 that the initial wave propagates without change of its initial profile and with the constant velocity $v_C = 0.97$ cells/normalized time unit (i.e., $V_C = 460$ cells/ps), as illustrated in Fig. 7, where the evolution of the compact solitary wave at 0, 80, and 170 normalized time is shown. The velocities issued from analytical and numerical analysis present a small discrepancy, which is remarkable because approximations have been made from Eq. (6) to Eq. (36). This behavior confirms the description of bright compact solitary in a DNA doubled strand with the extended NLS equation (9), corresponding to energy wave transfer in DNA molecules. The energy is localized in a limited narrow region for biologically significant duration and can propagate as the bright compacton and a large part of the energy is stored in the hydrogen bonds. Note that a similar result for topological soliton with compact support was obtained by Saccomandi [19,20] in the context of an anharmonic lattice where the nonlinear dispersion is invoked to describe the dynamic of the system. Our results with compact support are in agreement with the result of these preceding studies. It is also interesting to check if a multicompacton solution of Eq. (29) such as

$$\phi(z) = B_0 \cos \mu(n - n_0), \text{ if } |(n - n_0)| \leqslant \pi/\mu \qquad (42)$$

can propagate and stays stable. In Fig. 8 two compactons move with a stable shape to the right with the same velocity, and for $-1 \leqslant C_{nl} \leqslant -0.4$; Fig. 9 demonstrates the emergence of stable compactons out of more general initial data. The emerging compactons are stable and preserve their initial shape. For the original Rosenau and Hyman [7] compacton equations, numerical investigations showed some remarkable properties, namely, whatever initial compact data were given, they eventually evolved into compactons. We show in Fig. 10

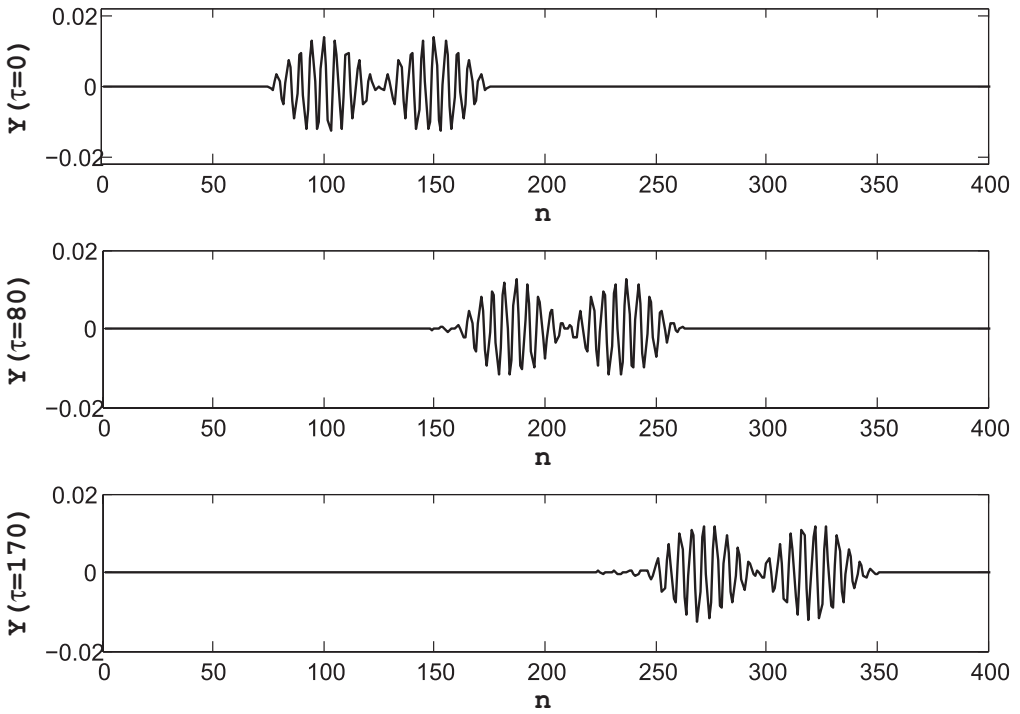

FIG. 8. Time behavior of multicompacton propagation in DNA. We use the parameter $C_{nl} = -0.4$, i.e., $\Delta H_n/C = 0.22\,\text{eV}$ and $b = 8\text{Å}^{-2}$. The propagation is stable along the DNA lattice.

that an initial compact wave decomposes into a sequence of compactons whose number depends on the initial energy. Notably for large energy, two emitted compactons appear and propagate to the left. From Figure 10 we see that even if the widths of the emitted compactons are small, they propagate keeping their stability. This suggests that for the case of a nonzero initial velocity, the stability of the compact wave does not depend on their width and amplitude. This may be

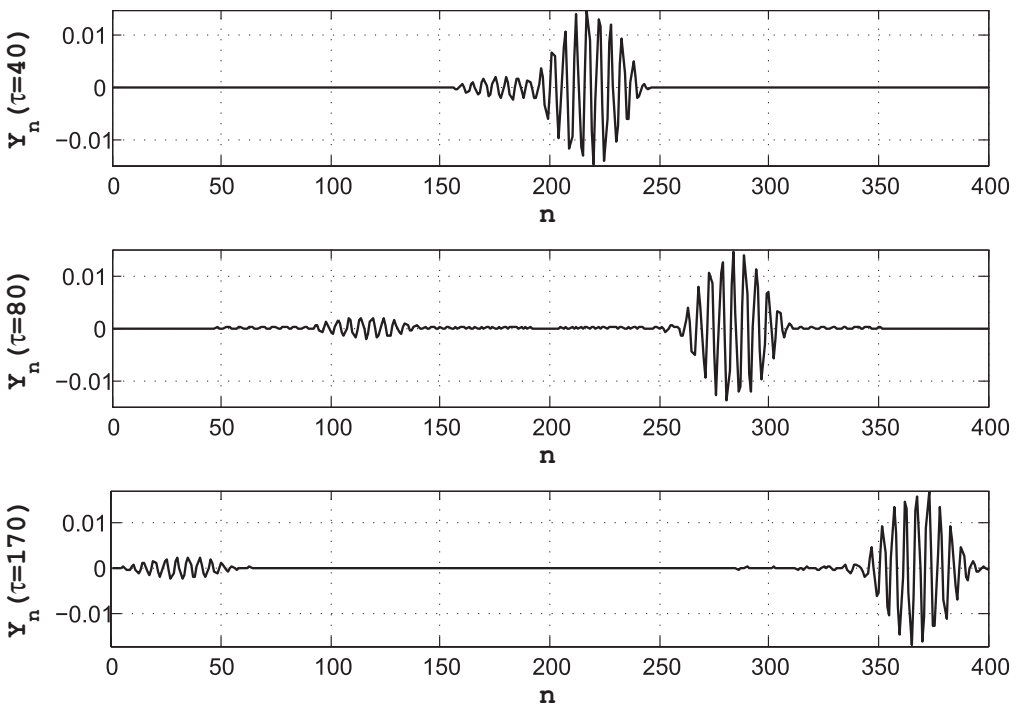

FIG. 9. Same as in Fig. 7, but the anharmonic parameter is $Cnl = -0.84$, i.e., $\Delta H_n/C = 0.1\text{eV}$ and $b = 8\text{Å}^{-2}$. The initial compacton preserves its shape but emits another compacton with a lower amplitude that propagates leftward with a conserved shape.

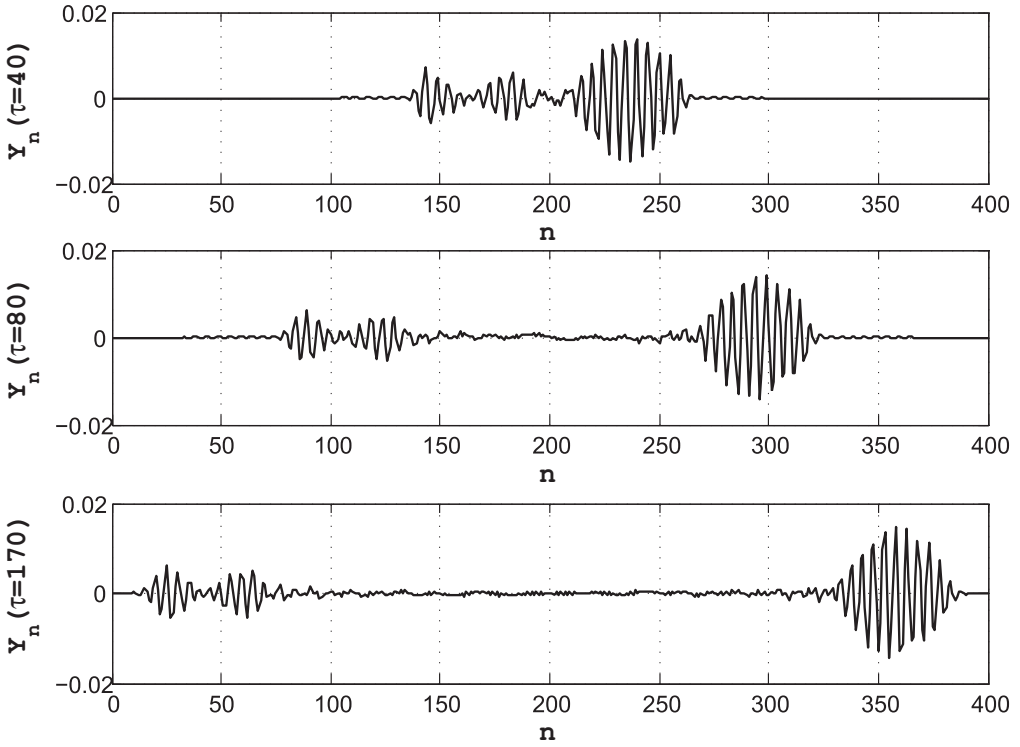

FIG. 10. Decomposition of an initial compacton for the parameter $Cnl = -0.9$, i.e., $\Delta H_n/C = 0.09\,\text{eV}$ and $b = 9\text{Å}^{-2}$. An initial compact wave breaks into a string of compactons, each of them remaining then stable.

understandable because the energy is contained in a moving compact region when a deliberately perturbed compact bright solitary wave with nonzero initial velocity is numerically tested. Even if the localized energy tends to be shared in the whole system, the wave stays very robust, as shown in Fig. 11.

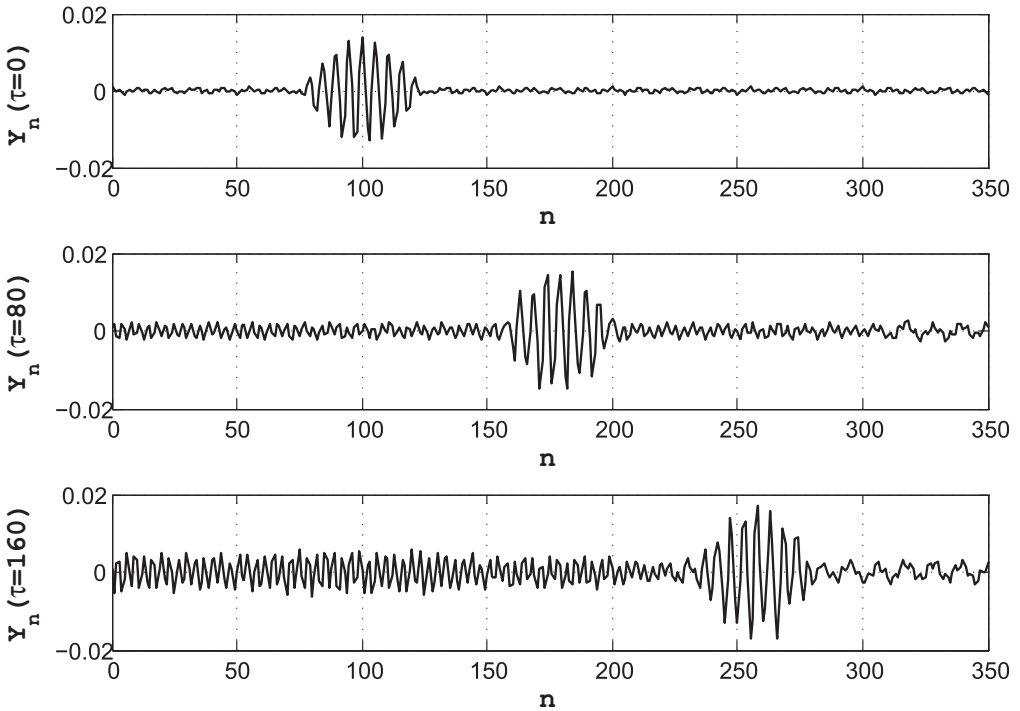

FIG. 11. Time evolution of a perturbated moving compact solitary wave, ($A = 0.016$ and $L = 50$), modulated with a wave number $q = 0.5\pi$. The perturbated compact solitary wave is stable during the displacement.

V. CONCLUSIONS

In this paper we have derived an extended NLS equation governing the dynamics of modulated waves in DNA lattice with nonlinear dispersion. This equation reduces to the standard NLS equation in the absence of nonlinear dispersion of the network. We have shown that this equation allows to successfully describe the propagation of envelope bright solitary wave with compact support. Numerical experiments have been carried out in order to confirm the analytical predictions. It has been observed that the existence and stability of the envelope bright compacton with zero velocity, in the nonlinear lattice with finite stacking energy, depends specially on the value of the amplitude. Otherwise, we have suggested that for the case of a nonzero initial velocity, the stability of the compact wave does not depend on its amplitude or width. Compact initial data stay stable or decompose into a train of stable compactons whose width depends on the number of emitted compactons. For the physical point of our work, by showing the existence and the stability of compact bright solitary waves in DNA, we provide a possible physical mechanism for the effect of finite enthalpy stacking on DNA dynamics. This model with on site-dependent finite stacking is used here to show the existence of a compact bright solitary wave in DNA double strands. This stacking interaction provides both the linear and nonlinear coupling parameters, which are fixed independently and control the dynamic and the stability of the system. As described in some detail in Ref. [12], this model can also provide the description of the physics of DNA melting and show that the finite enthalpy can also be responsible of the denaturation of DNA. We believe that this work shows a new vision on the concept of compactification of nonlinear waves in DNA and can also be exported in the study of many other physical systems. In the actual stage of the research on structures with compact support, it is true that the obtained results are still far away from practical applications. However a recent example reports that a specific terahertz radiation exposure may significantly affect the natural dynamics of DNA: Alexandrov *et al.* [26] choose the compact wave to be an effective perturbation for the creation of a localized unbinding state at an arbitrary point. Moreover, in order to measure the velocity of the soliton in the model of Peyrard-Bishop-Dauxois, Zdravkovic and Sataric [4] have proposed single-molecule experiments on the DNA molecule that might provide support to a couple of models describing the DNA dynamics and predicting the existence of nonlinear waves in DNA. In this context, theoretical studies can suggest interesting experiments in order to improve the physical knowledge of nonlinear waves in DNA. It is, however, important to point out that applications of these results in biology must be done with prudence. From a theoretical point of view, it is known that the stability and lifetime of localized solutions are very sensitive to properties of the thermal fluctuations such as viscosity and temperature [27–29]. The DNA is in contact with a thermal bath in the cell. Therefore, the friction and thermal forces play an important role in its internal dynamics. So it is necessary to explore the role of the thermal noise in the process of formation of these localized structures to study the creation and dynamics of localized structures in the JB model in a cell environment. On the other hand, such basic complex DNA functional processes as replication and transcription are controlled by means of the protein actions [30]. Therefore, to understand the DNA functioning, taking into account the internal interactions is necessary, but it should be completed by studying the interplay between the internal motion, e.g., internal oscillations in the DNA, and the proteins involved in the processes.

[1] M. Peyrard, Nonlinearity **17**, 1 (2004).
[2] M. Peyrard and A. R. Bishop, Phys. Rev. Lett. **62**, 2755 (1989).
[3] J. Deluca, E. Drigo Filho, A. Ponno, and J. R. Ruggiero, Phys. Rev. E **70**, 026213 (2004).
[4] S. Zdravkovic and M. V. Sataric, Phys. Rev. E **77**, 031906 (2008).
[5] R. Gonzalez, Y. Zeng, V. Ivanov, and G. Zocchi, J. Phys. Condens. Matter **21**, 034102 (2009).
[6] C. B. Tabi, A. Mohamadou, and T. C. Kofané, Phys. Lett. A **373**, 3801 (2009).
[7] P. Rosenau and J. M. Hyman, Phys. Rev. Lett. **70**, 564 (1993).
[8] A. Pikovsky and P. Rosenau, Physica D **218**, 56 (2006).
[9] A. S. T. Nguetcho, P. B. Ndjoko, and T. C. Kofané, Eur. Phys. J. B **62**, 7 (2008).
[10] A. S. T. Nguetcho and T. C. Kofané, Eur. Phys. J. B **57**, 411 (2007).
[11] T. Dauxois, M. Peyrard, and A. R. Bishop, Phys. Rev. E **47**, 684 (1993).
[12] M. Joyeux and S. Buyukdagli, Phys. Rev. E **72**, 051902 (2005).
[13] M. Joyeux, S. Buyukdagli, and M. Sanrey, Phys. Rev. E **75**, 061914 (2007).
[14] T. Dauxois, M. Peyrard, and A. R. Bishop, Phys. Rev. E **47**, R44 (1993).
[15] D. Yemélé and F. Kenmogne, Phys. Lett. A **373**, 3801 (2009).
[16] Y. S. Kivshar and M. Peyrard, Phys. Rev. A **46**, 3198 (1992).
[17] M. Peyrard, T. Dauxois, and C. Willis, in *Nonlinear Coherent Structures in Physics and Biology*, edited by K. H. Spatschek and F. G. Mertens (NANO Advanced Studies Institute Series B: Physics, Plenum Press, New York, 1994), Vol. 329, pp. 29–38.
[18] D. Yemélé, P. Marquié, and J. M. Bilbault, Phys. Rev. E **68**, 016605 (2003).
[19] G. Saccomandi and I. Sgura, J. R. Soc. Interface **3**, 655 (2006).
[20] G. Saccomandi, Int. J. Non-Lin. Mech. **39**, 331 (2004).
[21] P. Tchofo Dinda and M. Remoissenet, Phys. Rev. E **60**, 6218 (1999).
[22] G. Gaeta, T. Gramchev, and S. Walcher, J. Phys. A: Math. Theor. **40**, 4493 (2007).
[23] F. Cooper, J. M. Hyman, and A. Khare, Phys. Rev. E **64**, 026608 (2001).
[24] M. Eleftheriou, B. Dey, and G. P. Tsironis, Phys. Rev. E **62**, 7540 (2000).

[25] A. V. Gorbach and S. Flach, Phys. Rev. E **72**, 056607 (2005).
[26] B. Alexandrov, V. Gelev, A. Bishop, A. Usheva, and K. Ø. Rasmussen, Phys. Lett. A **374**, 1214 (2010).
[27] R. M. Haas, Phys. Rev. D **57**, 7422 (1998).
[28] E. Zamora-Sillero, A. V. Shapovalov, and F. J. Esteban, Phys. Rev. E **76**, 066603 (2007).
[29] J. J.-L. Ting and M. Peyrard, Phys. Rev. E **53**, 1011 (1996).
[30] C. R. Calladine and H. R. Drew, *Understanding DNA* (Academic, London, 2002).